are being utilized. Details of this work will be published separately.

It is a pleasure to express my thanks to the University of London for the award of an I.C.I. Fellowship, during the tenure of which this work was carried out.

References

ABRAHAMS, S. C. (1955). *Acta Cryst.* **8**, 661.
ABRAHAMS, S. C., ROBERTSON, J. M. & WHITE, J. G. (1949). *Acta Cryst.* **2**, 233, 238.
BERGHUIS, J., HAANAPPEL, IJ. M., POTTERS, M., LOOPSTRA, B. O., MACGILLAVRY, C. H. & VEENENDAAL, A. L. (1955). *Acta Cryst.* **8**, 478.
BRILL, R. (1950). *Acta Cryst.* **3**, 333.
BROWN, C. J. (1953). *J. Chem. Soc.* p. 3278.
BUERGER, M. J. (1941). *Numerical Structure Factor Tables.* Geological Society of America, Special Papers No. 33.
COCHRAN, W. (1951). *Acta Cryst.* **4**, 81.
COCHRAN, W. (1953). *Acta Cryst.* **6**, 260.
COCHRAN, W. (1954). *Acta Cryst.* **7**, 503.
COX, E. G., CRUICKSHANK, D. W. J. & SMITH, J. A. S. (1955). *Nature, Lond.* **175**, 766.
GILBERT, R. E. & LONSDALE, K. (1956). *Acta Cryst.* **9**, 697.
HOERNI, J. A. & IBERS, J. A. (1954). *Acta Cryst.* **7**, 744.
HUGHES, E. W. (1941). *J. Amer. Chem. Soc.* **63**, 1737.
International Tables for X-ray Crystallography (1952), vol. 1. Birmingham: Kynoch Press.
JAMES, R. W. & BRINDLEY, G. W. (1931). *Z. Kristallogr.* **78**, 470.
JEFFREY, G. A. & CRUICKSHANK, D. W. J. (1953). *Quart. Rev. Chem. Soc., Lond.* **7**, 335.
LEVY, H. A. (1954). *Acta Cryst.* **7**, 617, 690.
LIPSON, H. & COCHRAN, W. (1953). *The Determination of Crystal Structures.* London: Bell.
MCWEENY, R. (1951). *Acta Cryst.* **4**, 513.
RADOSLOVITCH, E. W. & MEGAW, H. D. (1955). *Acta Cryst.* **8**, 95.
ROLLETT, J. S. (1955). *Acta Cryst.* **8**, 487.
ROLLETT, J. S. & DAVIES, D. R. (1955). *Acta Cryst.* **8**, 125.
VAUGHAN, P. & DONOHUE, J. (1952). *Acta Cryst.* **5**, 530.
WILSON, A. J. C. (1942). *Nature, Lond.* **150**, 152.

Acta Cryst. (1956). **9**, 721

The Morphology of Zircon and Potassium Dihydrogen Phosphate in Relation to the Crystal Structure

BY P. HARTMAN

Kristallografisch Instituut der Rijksuniversiteit, Melkweg 1, *Groningen, Netherlands*

(*Received* 21 *March* 1956)

The periodic bond chain theory of crystal morphology is applied to zircon. The lattice energy and the attachment energies of several faces are calculated, assuming an ionic structure with Zr^{4+} and SiO_4^{4-} ions. Corrections are made for the tetrahedral shape of the silicate ion. In general a higher attachment energy corresponds to lower *P*- and *F*-values (persistences) of the forms.

The most important zones are [001], [100] and [111]. An explanation is given of their development.

The electrostatic lattice energy and the attachment energies of (010) and (011) of KH_2PO_4 are calculated.

A 'theoretical habit' is derived for zircon and for KH_2PO_4; the agreement with the observed habit is good.

The growth fronts on (010) of KH_2PO_4 parallel to [100] are explained in terms of growth controlled by surface migration.

Introduction

Recently, a method was proposed of deriving the morphology of crystals from the crystal structure (Hartman & Perdok, 1955*a*, *b*). This method will be applied to the zircon type of crystal structure, which is found, for instance, in zircon, KH_2PO_4, scheelite, wulfenite, $KReO_4$ and so on. The structures of these substances are closely related, as regards positions and coordination of atoms, although they belong to different space groups. First, the morphology of zircon will be treated in detail, and then some remarks will be made on the morphology of KH_2PO_4.

Morphology of zircon

The relative morphological importance of the forms is given by the *Kombinationspersistenz* (*P*-value) and the *Fundortspersistenz* (*F*-value) (cf. Niggli, 1923). These quantities were obtained from an inspection of 129 figures appearing in Goldschmidt's *Atlas der Krystallformen* (1923), which gave 43 different ob-

served combinations of forms and 49 different localities. The P- and F-values of the observed forms are given in Table 1; the indices refer to the body-centred

Table 1. *P- and F-values of zircon*

	Form	P	F	Number of times that the form is the largest one
s	{011}	88	96	34
m	{010}	77	88	43
a	{110}	58	75	37
λ	{211}	58	65	4
π	{031}	35	41	2
e	{112}	33	35	6
g	{021}	21	20	2
ω	{321}	12	10	0
ψ	{532}	12	6	0
c	{001}	12	4	0
β	{012}	7	2	1

Forms that are qualified as rare or uncertain have been omitted.

lattice. The numbers in the last column of Table 1 indicate on how many figures out of 129 a certain form is the largest of all.

Bonds and periodic bond chains in zircon

Zircon, $ZrSiO_4$, crystallizes in the space group $I4/amd$–D_{4h}^{19}, with $c = 5{\cdot}88$ Å, $a = 6{\cdot}60$ Å. The positions of the zirconium atoms and the silicon atoms is given in Table 2.

Table 2. *Positions of* Zr *and* Si *atoms in zircon*

Zr(1)	0, 0, 0	Si(1)	0, 0, $\frac{1}{2}$
Zr(2)	0, $\frac{1}{2}$, $\frac{1}{4}$	Si(2)	0, $\frac{1}{2}$, $\frac{3}{4}$
Zr(3)	$\frac{1}{2}$, $\frac{1}{2}$, $\frac{1}{2}$	Si(3)	$\frac{1}{2}$, $\frac{1}{2}$, 0
Zr(4)	$\frac{1}{2}$, 0, $\frac{3}{4}$	Si(4)	$\frac{1}{2}$, 0, $\frac{1}{4}$

In the following treatment it is assumed that the building units in the crystallization process are Zr^{4+} ions and SiO_4^{4-} ions. The silicate ions will be indicated by the position of the silicon atoms. Three different bonds can be distinguished:

(a) from Zr (0, 0, 0) to Si (0, 0, $\frac{1}{2}$);
(b) from Zr (0, 0, 0) to Si ($\frac{1}{2}$, 0, $\frac{1}{4}$);
(c) from Zr (0, 0, 0) to Si ($\frac{1}{2}$, $\frac{1}{2}$, 0).

The first and second of these are strong bonds between ions in the first coordination sphere. The third bond is weaker and as a first approximation it might be neglected. It is, however, introduced here, because it allows a more detailed treatment.

The three bonds allow the construction of many periodic bond chains, but only those given in Table 3 appear to be necessary to account for the observed morphology. The result is not changed when further periodic bond chains are considered.

The four periodic bond chains and their symmetrical equivalents allow five possible F-forms, namely {010}, {011}, {001}, {110} and {112}. The faces of all these forms are parallel to two or more periodic bond chains

Table 3. *Periodic bond chains of zircon*

Periodic bond chain	Direction*	Atoms that belong to one period
A	[001]	Zr(0, 0, 0)–Si(0, 0, $\frac{1}{2}$)–Zr(0, 0, 1)
B	[100]	Zr(0, 0, 0)–Si($\frac{1}{2}$, 0, $\frac{1}{4}$)–Zr(1, 0, 0)
C	[$\frac{1}{2}\frac{1}{2}\frac{1}{2}$]	Zr(0, 0, 0)–Si($\frac{1}{2}$, 0, $\frac{1}{4}$)–Zr($\frac{1}{2}$, $\frac{1}{2}$, $\frac{1}{2}$)
D	[110]	Zr(0, 0, 0)–Si($\frac{1}{2}$, $\frac{1}{2}$, 0)–Zr(1, 1, 0)

* The general symbol [uvw] is used to indicate a zone direction as well as a distance between identical points.

and it will be shown that they are 'genuine' F-faces, that is to say, they satisfy the conditions that (1) the whole structure can be divided into slices parallel to these faces, and (2) the profile of such a slice does not contain elements of slices of other F-faces. The morphology will be treated zone after zone.

The development of the zone [001]

The F-forms in this zone are {010} and {110}.

(a) {010}.—The structure can be divided parallel to (010) into slices with stoichiometric composition (Fig. 1(a)). The Zr and Si atoms of these slices are coplanar. The morphological importance of this face depends on its attachment energy, to the calculation of which we

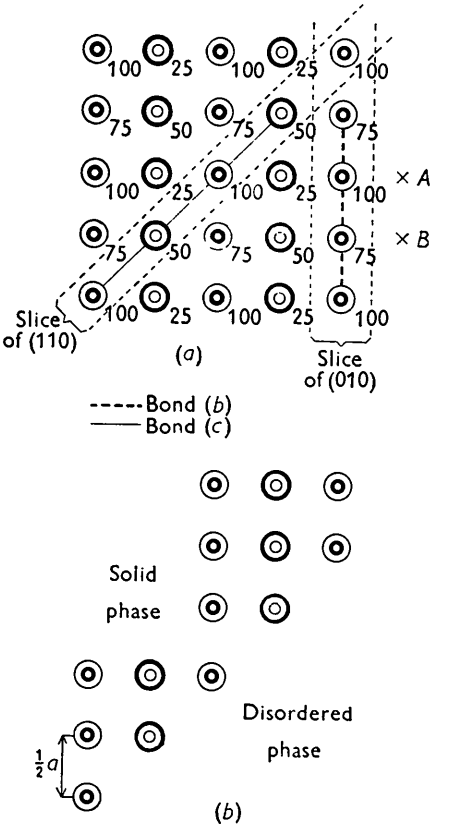

Fig. 1. (a) Projection of the zircon structure on (001). Small circles: Zr ions. Large circles: silicate ions. The heights of the Zr ions are indicated; the Si atoms lie at a distance $\frac{1}{4}c$ above and below the Zr ions. (b) Profile of the face (110), projected on (001).

now proceed. The zircon and silicate ions are considered as point charges. The structure is divided into a set of parallel periodic bond chains [001]. The electrostatic potential at a point at a certain distance from such a chain of ions can be calculated by means of the formulas of Madelung (1918) and Kleber (1939). The electrostatic potential in the site of a Zr ion with respect to the nearest (010) layer is then obtained by adding the separate contributions of all chains [001] in that layer. The value of this potential is $V_1 = (4e/c) \times -0{\cdot}0603$ Å^{-1}, in which e is the electronic charge and $c = 5{\cdot}88$ Å. The second nearest layer has a contribution to the potential equal to $V_2 = (4e/c) \times +0{\cdot}0038$ Å^{-1}. The contribution of other layers is negligible. The potentials in the site of a silicate ion have the same value as in the site of a Zr ion. Hence the attachment energy per molecule, taking into account the actual charges of the ions, becomes: $E_{010} = 8(V_1 + V_2) = -0{\cdot}307$ e.^{2}Å^{-1}.

For the calculation of attachment energies of other faces it is convenient to know the lattice energy. Therefore we calculate the electrostatic energy in the zero layer of (010). The contribution of the zero chain to the electrostatic potential is $V_0' = -(4e/c) \ln 16$; the other chains contribute $V_0'' = (4e/c) \times +0{\cdot}0063$. The electrostatic energy of the whole layer becomes $E_0(010) = 8(V_0' + V_0'') = -15{\cdot}055$ e.^{2}Å^{-1} per molecule. The lattice energy thus becomes:

$$E_{\text{lattice}} = \tfrac{1}{2}\{E_0(010) + 2E_{010}\} = -7{\cdot}835 \text{ e.}^2\text{Å}^{-1} \text{ per molecule.}$$

(*b*) {110}.—The whole structure can be divided into neutral slices parallel to (110) (Fig. 1(*a*)), so that this face satisfies the first condition for *F*-faces. It is questionable whether or not the second condition is satisfied and we return to this problem in a later section.

The electrostatic energy of the zero layer is found to be $E_0(110) = -15{\cdot}417$ e.^{2}Å^{-1} per molecule, so that the attachment energy becomes $E_{110} = E_{\text{lattice}} - \tfrac{1}{2}E_0(110) = -0{\cdot}127$ e.^{2}Å^{-1} per molecule.

The energy values calculated so far have been obtained by considering the silicate ion as a point charge. This can be done, when the silicate ion is not too close to the point in which the potential is calculated, but we have to introduce corrections for the potential energy of silicate ions in the first coordination sphere. The exact positions of the oxygen atoms are not determined, but we assume the silicate ion to be tetrahedral in shape with an Si–O distance of 1·60 Å. The oxygen atoms are given a charge −2 and the silicon atom a charge +4. The correction for the electrostatic energy between the zirconium atom (1) and the silicate ion (1) (see Table 2 for their positions) amounts to $\Delta_1 = +0{\cdot}10$ e.^{2}Å^{-1} per ion. The correction for the interaction of Zr(1) with silicate ion (4) is $\Delta_2 = -0{\cdot}49$ e.^{2}Å^{-1} per ion and for the interaction of the two silicate ions (1) and (4) the correction is found to be $\Delta_3 = -0{\cdot}44$ e.^{2}Å^{-1} per ion. Per molecule the following corrections have to be applied:

to the lattice energy: $2\Delta_1 + 4\Delta_2 + 2\Delta_3 = -2{\cdot}64$ e.^{2}Å^{-1};
to the attachment energy of (010): $2\Delta_2 + \Delta_3 = -1{\cdot}42$ e.^{2}Å^{-1};
and to the attachment energy of (110): $4\Delta_2 + 2\Delta_3 = -2{\cdot}84$ e.^{2}Å^{-1}.

With these corrections the lattice energy becomes $-10{\cdot}47$ e.^{2}Å^{-1} per molecule, and the attachment energies of (010) and (110) become respectively $-1{\cdot}73$ and $-2{\cdot}97$ e.^{2}Å^{-1} per molecule. The attachment energy of (010) is the smaller one, which means that this face is more important than (110), as is actually observed: the persistences (*P*-values and *F*-values, cf. Table 1) of (010) are higher than those of (110).

(*c*) *Other forms* {*hk*0}.—The attachment energy of all these forms is the same, because they are all *S*-forms. The uncorrected electrostatic energy of the periodic bond chain [001] is $E_{[001]} = -(32e/c) \ln 16 = -15{\cdot}089$ e.^{2}Å^{-1} per molecule. The attachment energy is equal to the difference between the lattice energy and half the energy of the periodic bond chain; in this case it amounts to $-0{\cdot}29$ e.^{2}Å^{-1}. The corrections to be applied are: $4\Delta_2 + 2\Delta_3 = -2{\cdot}84$ e.^{2}Å^{-1}, so that the attachment energy of an *S*-face in the zone [001] becomes $-3{\cdot}13$ e.^{2}Å^{-1} per molecule, which is higher than E_{010} and E_{110}. These *S*-faces have therefore a greater displacement velocity than the *F*-faces (010) and (110). None of them has been observed.

The development of the zone [100]

The *F*-forms in this zone are {010}, {011}, and {001}.

(*a*) {011}.—The whole structure can be divided into slices parallel to (011). Fig. 2(*a*) shows such a slice, which consists of two consecutive layers of positively and negatively charged ions. Ions of both layers are bound to ions of other slices lying beneath. The attachment energy can be calculated by first calculating the electrostatic energy of a complete slice. This is carried out in the same way as the calculation of the energy of a (111)-slice of sphalerite (Hartman, 1956). We find $E_0(011) = -12{\cdot}031$ e.^{2}Å^{-1} per molecule, from which follows the attachment energy $E_{011} = -1{\cdot}82$ e.^{2}Å^{-1}. The correction to be applied amounts to $2\Delta_1 + \Delta_2 + 2\Delta_3 = -1{\cdot}17$ e.^{2}Å^{-1}, so that the final value is $E_{011} = -2{\cdot}99$ e.^{2}Å^{-1} per molecule.

(*b*) {001}.—In this case each slice consists of one layer, the distance between the layers being $\frac{1}{4}c$ (Fig. 2(*a*)). The energy of one slice is $E_0(001) = -11{\cdot}074$ e.^{2}Å^{-1}, from which follows the attachment energy $E_{001} = -2{\cdot}30$ e.^{2}Å^{-1}. The correction amounts to $2\Delta_1 + 4\Delta_2 + 2\Delta_3 = -2{\cdot}64$ e.^{2}Å^{-1} so that the final value is $E_{001} = -4{\cdot}94$ e.^{2}Å^{-1} per molecule.

(*c*) *S-faces.*—The electrostatic energy per molecule in a periodic bond chain [100] is $E_0[100] = -11{\cdot}666$ e.^{2}Å^{-1}. The attachment energy is $E_{[100]} = E_{\text{lattice}} - \tfrac{1}{2}E_0[100] = -2{\cdot}00$ e.^{2}Å^{-1}; the correction amounts

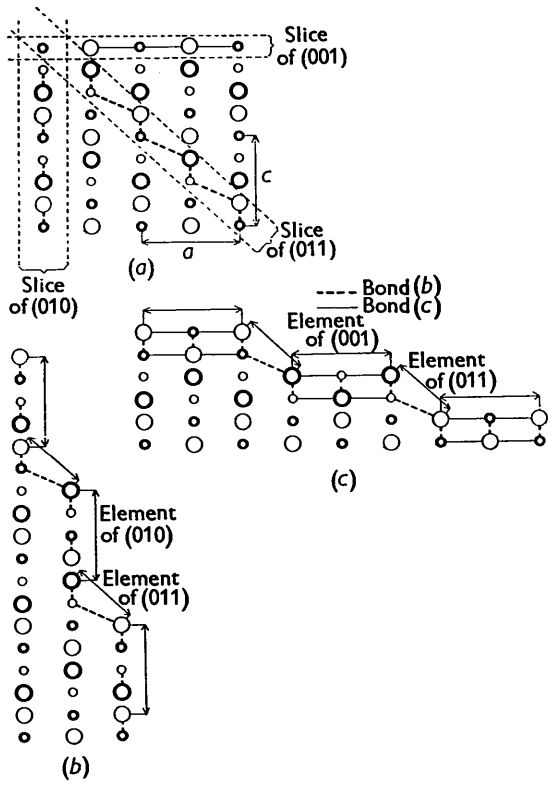

Fig. 2. Projection of the zircon structure on (100). (*a*) The slices of the *F*-faces; bonds *a* are not shown. (*b*) Profile of the S_1-face (031). (*c*) Profile of the S_1-face (013). Small circles: Zr ions; large circles: silicate ions.

to $2\Delta_1+2\Delta_2+2\Delta_3 = -1{\cdot}66$ e.^{2}Å^{-1}, so that the final value is $-3{\cdot}66$ e.^{2}Å^{-1}.

The first *S*-face between the *F*-faces (010) and (011) shows a profile that consists of alternating elements (strips) of these faces. The periodic bond chains in a slice of (010) are repeated with a period [001]; those in a slice of (011) are repeated with a period $[\frac{1}{2}\bar{\frac{1}{2}}\frac{1}{2}]$. The chains in the first *S*-face are repeated, therefore, with a period $[001]+[\frac{1}{2}\bar{\frac{1}{2}}\frac{1}{2}] = [\frac{1}{2}, \bar{\frac{1}{2}}, \frac{3}{2}]$, so that the indices of this S_1-face become (031) (cf. Fig. 2(*b*)). Similarly the profile of the face (021) consists of two elements of (011) alternating with one element of (010).

The addition scheme of indices reads:

F-faces	(020)			(011)
S_1-face		(031)		
S_2-face	(051)		(042)	

According to the periodic bond chain theory the S_1-face should be more important than the *S*-faces. Indeed (031) has a *P*-value 35, which exceeds the *P*-value 21 of (021). The face (051) is very rare.

The second part of the zone between (011) and (001) shows two remarkable features: (*a*) Only the *S*-face (012) has been observed and it has the low *P*-value 7. (*b*) The attachment energy of the *F*-face (001) is $-4{\cdot}94$ e.^{2}Å^{-1} and it exceeds the attachment energy $-3{\cdot}66$ e.^{2}Å^{-1} of the *S*-faces.

Arguments will be given that probably a relation exists between these two features. The only way in which it is possible that an *F*-face has a higher attachment energy than an *S*-face is that the *F*-face grows in slices which do not contain the periodic bond chain to which the *S*-face is parallel. A slice of (001) contains the periodic bond chains [110] and [1$\bar{1}$0], but it does not contain the chain [100] (see Fig. 2(*a*)). If the growth fronts on (001) are polygonized, they will therefore be parallel to [110] and [1$\bar{1}$0]. A slice of (011), on the other hand, does contain the chain [100]. Let us compare now the behaviour on growth of two S_n-faces.

The profile of the first one contains *n* elements of (001) and one element of (011) and the face can be symbolized by $S(\rightarrow 001)$. The profile of the second face contains *n* elements of (011) and one element of (001), and it can be symbolized by $S(\rightarrow 011)$. Now, if $S(\rightarrow 001)$ would be an ordinary *S*-face, it would grow by first filling up one chain [100], then a second chain [100], and so on. But because the attachment energy of (001) is higher than that of an *S*-face in the zone [100], it is more probable that a new slice of (001) starts growing at the step edge of $S(\rightarrow 001)$, till the whole flat part is covered. Then a new slice starts at the edge, and so on. The face $S(\rightarrow 001)$ grows, therefore, in a way that is comparable with that of the face (001), so that the displacement velocity of $S(\rightarrow 001)$ will be enhanced. In the case of $S(\rightarrow 011)$ the enhancement will be much smaller, because there is only one element of (001) against *n* elements of (001). Hence the conclusion is reached that the *S*-faces between (011) and (001) have an increased displacement velocity, the increase being smaller for faces near (011) and greater for faces near (001).

The indices of the S_1-face can be derived in the usual way, because it is only the profile that determines a face as an S_1-face or an S_2-face.

The periodic bond chains [100] in the face (001) are repeated with a period [0$\bar{1}$0]. The corresponding period in (011) was $[\frac{1}{2}\bar{\frac{1}{2}}\frac{1}{2}]$, so that the profile of the S_1-face has the period $[\frac{1}{2}, \bar{\frac{3}{2}}, \frac{1}{2}]$, which leads to the indices (013) for this face (Fig. 2(*c*)). The profile of the observed face (012) consists of two elements of (011) alternating with one element of (001). Theoretically, the face (013), being an S_1-face, would be expected to have a higher *P*-value than the S_2-face (012). Presumably the high attachment energy of (001) increases the displacement velocity of (012) less than that of (013), because the profile of (012) contains two elements of (011).

Development of the zone [$\bar{1}$11]

This zone contains the *F*-faces (110), (101), and (1$\bar{1}$2).

(*a*) (1$\bar{1}$2).—The structure can be divided parallel to this face into slices (cf. Fig. 3) that contain coplanar

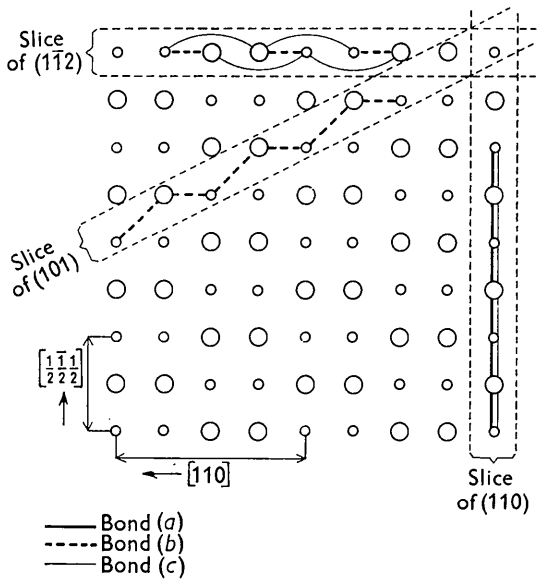

Fig. 3. Projection of the zircon structure on a plane perpendicular to [$\bar{1}$11]. A small circle represents a pile of Zr ions, a large circle a pile of silicate ions.

Zr and Si atoms. The easiest way to calculate the electrostatic energy of this slice is to start with the periodic bond chains [110].

We find: $E_0(112) = -8{\cdot}644$ e.^{2}Å^{-1} per molecule, which gives the attachment energy $E_{112} = -3{\cdot}51$ e.^{2}Å^{-1}. The correction amounts to $2\Delta_1+2\Delta_2+\Delta_3 = -1{\cdot}22$ e.^{2}Å^{-1}, so that the final value becomes $-4{\cdot}73$ e.^{2}Å^{-1}.

(*b*) *S-faces.*—The electrostatic energy per molecule in a periodic bond chain [111] is $E_0[111] = -12{\cdot}468$ e.^{2}Å^{-1}. The attachment energy of *S*-faces in this zone is $E_{[111]} = E_{\text{lattice}} - \frac{1}{2}E_0[111] = -1{\cdot}60$ e.^{2}Å^{-1}.

The correction amounts to $2\Delta_1+2\Delta_2+2\Delta_3 = -1{\cdot}66$ e.^{2}Å^{-1}, which leads to the final value $E_{[111]} = -3{\cdot}26$ e.^{2}Å^{-1}.

The periodic bond chains in the face (110) are repeated with a period [$\frac{1}{2}$, $\frac{\bar{1}}{2}$, $\frac{1}{2}$] (cf. Fig. 3) and in (101) with a period [0, $\bar{1}$, 0], so that the profile of the S_1-face has the period [$\frac{1}{2}$, $\frac{\bar{3}}{2}$, $\frac{1}{2}$], which leads to the indices (211). The addition scheme of indices reads:

F-faces	(110)		(101)
S_1-face		(211)	
S_2-faces	(321)		(312)

The S_1-face (211) has a *P*-value 58, which exceeds the value 12 of (321). The face (312) has not been observed. One S_3-face has been observed: (532) with a *P*-value 12.

The second part of the zone, between (101) and (1$\bar{1}$2) shows the same feature as the zone [100] between (011) and (001). Here the attachment energy, $-4{\cdot}73$ e.^{2}Å^{-1} of (1$\bar{1}$2), is greater than that of the *S*-faces: $-3{\cdot}26$ e.^{2}Å^{-1}. Consequently the displacement velocity of the *S*-faces will be increased so that their *P*-values will be small. No *S*-faces are observed in this part of the zone.

Development of the zone [110]

This zone contains three *F*-forms {001}, {112} and {110}, but *S*-forms are very rare. Indeed, the attachment energy of these is large: the electrostatic energy per molecule in one periodic bond chain [110] is $E_0[110] = -9{\cdot}506$ e.^{2}Å^{-1}, from which: $E_{[110]} = -3{\cdot}08$ e.^{2}Å^{-1}. The correction is $2\Delta_1+4\Delta_2+2\Delta_3 = -2{\cdot}64$ e.^{2}Å^{-1}, so that the final value is $E_{[110]} = -5{\cdot}72$ e.^{2}Å^{-1}.

Discussion

(1) *F-forms.*—In the derivation of the *F*-forms we used the weak bond between Zr(0, 0, 0) and Si($\frac{1}{2}$, $\frac{1}{2}$, 0), which introduced the periodic bond chain [110]. We found that parallel to (110) the whole structure can be divided into slices. Thus the profile of the (110)-face can be described as that of an *F*-face: the slices contain coplanar Zr and Si atoms and they are separated by a distance $\frac{1}{4}a\sqrt{2}$ (Fig. 1(*a*)).

However, a different description is equally well possible: the profile consists of alternating elements of (100) and (010). In (010) the periodic bond chains [001] are repeated with a period [$\frac{1}{2}$, 0, 0]. Owing to the action of the glide plane *a* the attachment energy of an ion remains the same, whether it is attached in a position *A* or a position *B* (cf. Fig. 1(*a*)). Therefore the element period of (010) is [$\frac{1}{2}$, 0, 0] and of (100) it is [0, $\frac{1}{2}$, 0]. Consequently the profile of (110) can also be considered as the profile of an S_1-face in the zone [001] (Fig. 1(*b*)). Here we encounter the limit of the possibilities of the periodic bond chain theory: the difference between the *F*- or *S*-character of a form can no longer be sharp when a certain *F*-face contains one kind of periodic bond chain the energy of which is much higher than that of periodic bond chains in other directions. In the present case the energy of a periodic bond chain [001], corrected for the tetrahedral shape of the silicate ions, is $-15{\cdot}09+4\Delta_1 = -14{\cdot}69$ e.^{2}Å^{-1} per molecule, which is rather high compared with the corresponding value $-9{\cdot}51$ for a periodic bond chain [110].

As can be seen from Table 4 an increased attachment energy of the *F*-forms corresponds to a lower *P*- or *F*-value, with the exception of the form {011}. The high *P*- and *F*-value of {011} can be understood, when the forms {010} and {110} are recognized as open forms. Among the closed forms, {011} is the most prominent one and in general it will be present, whatever the prism that is developed. Consequently the bipyramid {011} will have greater persistence values than the prisms. In general, the prisms are larger than the bipyramid, as is shown by the numbers in the last column of Table 1.

Table 4. *F-forms of zircon*

F-form	{011}	{010}	{110}	{112}	{001}
Attachment energy (e.²Å⁻¹ per molecule)	−2·99	−1·73	−2·97	−4·73	−4·94
P-value	88	77	58	33	12
F-value	96	88	75	35	4

(2) *'Theoretical habit'*.—If it is assumed that the displacement velocities of the *F*-faces are proportional to the attachment energies, a 'theoretical habit' can be constructed. It appears then, that zircon crystals are bounded by two forms only: {010} and {011}. The displacement velocities of the other *F*-forms are too great to allow them to be present on the crystals. Fig. 4(*a*) shows the theoretical habit, which agrees well with the habit commonly observed.

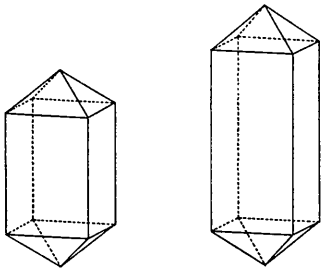

Fig. 4. 'Theoretical habit' of (*a*) zircon, (*b*) KH_2PO_4.

(3) *S-forms*.—It has been suggested (Hartman & Perdok, 1955*c*) that the occurrence of *S*-forms on minerals is due to alternating periods of growth and dissolution in an impure environment. Now it is not known which impurities are responsible for the habit changes of zircon. Yet it may be possible to account for the following facts: (*a*) The zone [111] contains three *S*-forms, of which {211} has rather high *P*- and *F*-values. (*b*) The zone [100] contains also three *S*-forms, the *P*- and *F*-values of which are lower than in the former case. (*c*) *S*-forms in the zones [001] and [110] are very rare.

Recently Kern (1953*a*, *b*; 1955*a*, *b*) concluded, from a number of experiments on ionic crystals, that the habit changes produced by impurities are often the same as those produced by supersaturation. He also showed that the influence of supersaturation was such as to favour the development of faces with a high electrostatic field, or, in other words, faces that contain an outer layer, densely packed with equally charged ions (like the octahedron face of NaCl). These faces lie in zones that correspond to zigzag periodic bond chains with short periods.

Applying these results to zircon, we see that faces in the zone [111] are likely to be produced on habit change: the zone corresponds to a zigzag periodic bond chain with the shortest possible period, namely 5·52 Å. Next comes the zone [100] with the period 6·60 Å; the corresponding chain deviates less from a straight line than the chain [111], so that the *S*-faces in this zone will be less important, as is actually observed. The periodic bond chains [001] and [110] are straight, so that the development of *S*-faces is unlikely, and in fact they seldom occur.

These considerations are also applicable to the *F*-faces that do not occur on the theoretical habit. The forms {110} and {112} lie in the zone [111] and the form {001}, which has much smaller *P*- and *F*-values, lies in the zone [100].

Potassium dihydrogen phosphate

This substance crystallizes in the space group $I\bar{4}2d$–D_{2d}^{12} with $c = 6{\cdot}945$ Å and $a = 7{\cdot}434$ Å (Ubbelohde & Woodward, 1947). The arrangement of the potassium atoms and the phosphorus atoms is entirely the same as that of the Zr and Si atoms in zircon. The only difference concerns the positions of the oxygens. The building units in the process of crystallization are K^+ ions and $H_2PO_4^-$ ions. When these ions are considered as point charges, the same bonds and periodic bond chains are found as with zircon. The morphology is therefore expected to be the same. The calculation of the lattice energy and the attachment energies are carried out in the same way as with zircon. The results, expressed in units e.²Å⁻¹ per molecule, are:

$$E_{\text{lattice}} = -0{\cdot}4187;\ E_{010} = -0{\cdot}0208;\ E_{011} = -0{\cdot}0851\ .$$

These values are not corrected for the non-spherical shape of the $H_2PO_4^-$ ion. When the origin is put at a phosphorus atom, the coordinates of one of the oxygens are: $x = 0{\cdot}081$, $y = 0{\cdot}144$ and $z = 0{\cdot}139$ (West, 1930). The hydrogen atoms are statistically distributed over the oxygen atoms (Frazer & Pepinsky, 1953) and therefore we assume the oxygens to have an electrical charge $-\frac{3}{2}$ and the phosphorus atom a charge $+5$. We then obtain the following corrections, as in the case of zircon:

$\Delta_1 = -0{\cdot}013$; $\Delta_2 = -0{\cdot}016$; $\Delta_3 = -0{\cdot}032$ in units e.²Å⁻¹ per ion.

The corrected values of the attachment energies then become:

$E_{010} = -0{\cdot}021 + 2\Delta_2 + \Delta_3 = -0{\cdot}085$ e.²Å⁻¹ per molecule;

$E_{011} = -0{\cdot}085 + 2\Delta_1 + \Delta_2 + 2\Delta_3 = -0{\cdot}191$ e.²Å⁻¹ per molecule.

When the crystal grows from an aqueous solution, the hydrogen bonds need not be considered, because the surface will be hydrated, so that each oxygen atom

is bound to a water molecule by means of a hydrogen bond. The attachment of a $H_2PO_4^-$ ion involves the breaking of this hydrogen bond and the formation of a new one. Presumably, this new hydrogen bond will be slightly stronger, so that a net amount of energy results of 1–2 kcal. per mole. 1 kcal. equals 0·003012 Ne.^{2}Å^{-1}, where N is Avogadro's number, so that the correction for the hydrogen bond energy can be neglected. The theoretical habit, based on the assumption that the displacement velocities are proportional to the electrostatic attachment energies, is shown in Fig. 4(*b*).

Growth fronts on (010)

On a crystal of KH_2PO_4 growing in an aqueous solution, growth fronts on (010) can often be observed. Sometimes these fronts are polygonized. The fronts are then parallel to the direction [100] and move from the centre of the crystal towards the ends (cf. also Bunn & Emmett, 1949). This is in contradiction with the observations of Amelinckx (1952) on apatite. He found that polygonized growth fronts have about the same shape as the crystal face.

If this were to be generally valid, the polygonized growth fronts of KH_2PO_4 should have a rectangular shape with the longer side parallel to [001]. This is also very probable according to the periodic bond chain theory: the electrostatic energy of the chain [001] is

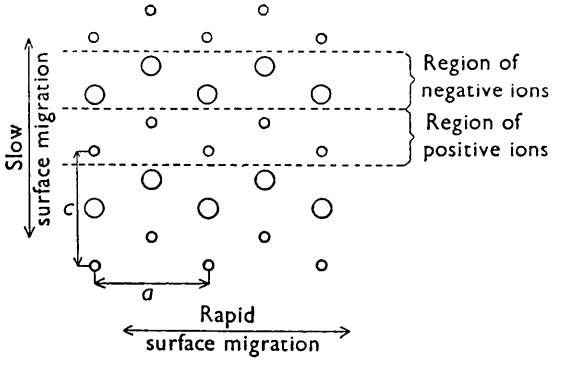

Fig. 5. Outer layer of (010) face.

$E_0[001] = -0{\cdot}798+4\Delta_1 = -0{\cdot}850$ e.^{2}Å^{-1} per molecule, which exceeds the corresponding value $E_0[100] = -0{\cdot}639+4\Delta_2 = -0{\cdot}703$ e.^{2}Å^{-1} per molecule.

If, however, the rates of advance of the growth fronts are controlled by surface diffusion, the shape will change. The surface of (010) can be described as consisting of narrow regions of positive ions, extending in the direction [100] with a width $\frac{1}{2}c$, alternating with similar regions of negative ions (Fig. 5).

An ion attached to the surface, can migrate relatively easily along the direction [100], sliding across ions of opposite sign. A migration along [001] is made difficult, because the ion has to cross a region occupied by ions of the same sign. Hence the growth front [001] will move forward with a much greater velocity than the growth front [100], so that the latter will persist.

The author wishes to express his thanks to Dr W. G. Perdok for his continuous interest and criticism.

References

Amelinckx, S. (1952). *Nature, Lond.* **170**, 760.

Bunn, C. W. & Emmett, H. (1949). *Disc. Faraday Soc.* No. 5, 119.

Frazer, B. C. & Pepinsky, R. (1953). *Acta Cryst.* **6**, 273.

Goldschmidt, V. (1923). *Atlas der Krystallformen.* Heidelberg: Winter.

Hartman, P. & Perdok, W. G. (1955*a*). *Acta Cryst.* **8**, 49.

Hartman, P. & Perdok, W. G. (1955*b*). *Acta Cryst.* **8**, 521.

Hartman, P. & Perdok, W. G. (1955*c*). *Acta Cryst.* **8**, 525.

Hartman, P. (1956). *Acta Cryst.* **9**, 569.

Kern, R. (1953*a*). *Bull. Soc. franç. Minér. Crist.* **76**, 325.

Kern, R. (1953*b*). *Bull. Soc. franç. Minér. Crist.* **76**, 393.

Kern, R. (1955*a*). *Bull. Soc. franç. Minér. Crist.* **78**, 461.

Kern, R. (1955*b*). *Bull. Soc. franç. Minér. Crist.* **78**, 497.

Kleber, W. (1939). *N. Jb. Min. Geol. Paläont,* Beil.-Bd. A, **75**, 72.

Madelung, E. (1918). *Phys. Z.* **19**, 524.

Niggli, P. (1923). *Z. Kristallogr.* **58**, 490.

Ubbelohde, A. R. & Woodward, I. (1947). *Proc. Roy. Soc.* A, **188**, 358.

West, J. (1930). *Z. Kristallogr.* **74**, 306.